

# IMPACT OF CARBOXYMETHYLATION PRETREATMENT ON THE MORPHOLOGICAL AND THERMAL CHARACTERISTICS OF CELLULOSE MICROFIBRILS FROM OIL PALM FROND TOWARD SOLAR THERMAL BENEFITS

MARSHAHIDA MAT YASHIM,\* MASITA MOHAMMAD,\*\* NUR AFRIZA BAKI,\*\*  
NILOFAR ASIM\*\* and AHMAD FUDHOLI\*\*

\*School of Chemical Engineering, College of Engineering, Universiti Teknologi MARA,  
23200 Dungun, Terengganu, Malaysia

\*\*Solar Energy Research Institute, Universiti Kebangsaan Malaysia, 43600 Bangi, Malaysia

\*\*\*Faculty of Computer and Mathematical Sciences, Universiti Teknologi MARA,  
23200 Dungun, Terengganu, Malaysia

✉ Corresponding author: M. Mohammad, masita@ukm.edu.my

Received October 17, 2022

The morphological and thermal characteristics of cellulose microfibril isolated from oil palm frond (OPF) waste, using carboxymethylation pretreatment, to benefit solar thermal application were explored. Following the pretreatments, 30 minutes of high-intensity ultrasonication (HIUS) at 20 kHz and 130 W output power were applied as a solvent-free fibrillation technique to produce cellulose microfibrils. The morphology of the isolated cellulose revealed that the consecutive techniques produced a long and uniform cellulose microfibril, with diameters ranging between 2 and 10  $\mu\text{m}$ , the coefficient of variation of its morphology distribution data being of 44.4%. It also caused the microfibril structure to shift from cellulose I to cellulose II, with a moderately high crystallinity index. Carboxymethylation greatly affected the thermal stability of cellulose microfibrils, with maximum degradation temperature up to 281  $^{\circ}\text{C}$ , as evident from TGA and DSC analyses. The surface chemistry for the carboxymethylated microfibril sample indicated significant changes in the functional groups responsible for its properties.

**Keywords:** waste minimization, biomass utilization, hydrodynamic forces, microfibril isolation, eco-friendly microfibrillation

## INTRODUCTION

Palm oil is the most widely used vegetable oil globally, accounting for up to 40% of total output, compared to other vegetable oils.<sup>1</sup> Since it was first introduced in the 14<sup>th</sup> century, palm oil production has become the key contributor to the economic sector of southeastern Asian countries, especially in the last decades. In 2014, the world's total oil palm production area was recorded at 16,472,000 ha, with Malaysia and Indonesia contributing 77 percent of this total, and the remaining were in Thailand, Nigeria and Columbia.<sup>2</sup> As palm oil production increases by around 9% per year globally,<sup>3</sup> the vast amount of biomass waste associated with the oil palm plantation is also growing. Environmentalists, academics, and society continue to be concerned

with managing and sustainably digesting this biomass waste,<sup>4</sup> and have developed various strategies for improving processes, procedures and environmental saving practices.

Wastes from pruning, replanting, and milling operations in oil palm plantations are often left to degrade on the fields, thereby exerting a detrimental impact on the environment. It was reported that palm oil only accounts for less than 10% of the tree, while the rest of the palm oil tree is considered biomass,<sup>5</sup> which includes oil palm trunk (OPT), oil palm frond (OPF), empty fruit bunch (EFB), oil palm kernel shell (OPKS), oil palm mesocarp fiber (OPMF) and palm oil mill effluent (POME).<sup>6</sup> OPF is produced daily from pruning activities and could cause substantial

hazards when left on the ground. Previous studies suggested an approach to directly convert OPF into value-added materials yet limited to animal feed, bioenergy production, organic fertilizer<sup>7</sup> and direct combustion to generate electricity.<sup>8,9</sup> The cellulose content in OPF ranges between 30.4 and 50.3%.<sup>10</sup> On a dry weight basis, OPF contains cellulose ( $35.73 \pm 1.34\%$ ), hemicelluloses ( $28.39 \pm 1.34\%$ ) and lignin ( $24.62 \pm 1.17\%$ ).<sup>11</sup> Exploiting the cellulose content from OPF through physical depolymerization could be leveraged to expand its potential for a sustainable supply of cellulose-based products, such as cellulose microfibrils, as a promising material for various energy-related applications.<sup>12</sup>

Microfiber's radiative cooling properties enable it to be inserted as a thermal insulating layer to create an efficient building cooling envelope effect.<sup>13</sup> Furthermore, microscale cellulose fibers are easily entangled with one another to form a highly flexible porous structure due to the high intermolecular affinity and strong hydrogen bonding, which has opened up their potential as thermal insulators in monolithic forms.<sup>14</sup> Recently, cellulose microfibrils have been converted into a three-dimensional aerogel to serve as a thermal insulator.<sup>15</sup> With the increasing need for environmentally friendly materials for solar thermal insulation technology, cellulose microfibrils are in great demand.<sup>16,17</sup> For this reason, there is a need for a process sequence to isolate cellulose and produce new materials with the desired qualities.

The characteristics of extracted cellulose were observed to be impacted not only by their native source, but also by the treatment processes used during fibrillation.<sup>18</sup> Several isolation techniques have been studied on various biomass resources in the past decades to extract cellulose microfibrils, including high-pressure homogenization,<sup>19,20</sup> high-shear homogenization,<sup>21,22</sup> micro-fluidization,<sup>23,24</sup> and mechanical grinding.<sup>25,26</sup> The mechanical fibrillation technique, like homogenization and micro-fluidization, could cause an irreversible agglomeration due to the hydrophilic nature of cellulose fibers. Hence, such methods frequently require multiple passes through disintegration devices, resulting in considerably high energy consumption.<sup>27</sup> It was estimated that the energy consumption required by a high-pressure homogenizer and micro-fluidization reaches as high as 70,000 kWh/t and 8.5 kWh, respectively.<sup>28</sup> High energy consumption due to a high-pressure operating

condition during homogenization has limited the scale-up of micron-sized production and caused its utilization for agricultural biomass to be less attractive.

Recently, high-intensity ultrasonication (HIUS) has been used to separate cellulose nanofibers, and it has received a lot of attention due to its capacity to degrade cellulosic polysaccharide bonds.<sup>29</sup> The ultrasonication method applies ultrasound energy at which hydrodynamic forces produce mechanical oscillating power. During ultrasonication, the alternating formation, growth and implosive collapse of bubbles (in a liquid medium) create highly intensive waves and hotspots to strip away the outer layer of cellulose and expose smaller fibril bundles. The cavitation process generates around 10-100 kJ/mol of energy, which falls within the hydrogen bond energy scale.<sup>30</sup> Besides being exceptionally clean, HIUS is also operationally convenient in reducing agglomerations during microfibrillation.

According to Fahma *et al.*, combining chemical and mechanical treatment produced the optimal conditions for manufacturing cellulose nanofiber from oil palm biomass.<sup>31</sup> Therefore, mechanical fibrillation techniques were usually combined with chemical pretreatments to ease the fibrillation and subsequently reduce its operating cost. TEMPO-mediated oxidation,<sup>32,33</sup> enzyme-assisted hydrolysis,<sup>34-36</sup> and ionic liquid treatments<sup>37</sup> are among the chemical treatments combined with mechanical fibrillation. Acid pretreatment is another profound chemical pretreatment method for obtaining nano-sized fibers from lignocellulosic biomass. The extracted cellulose is hydrolyzed using a mixture of hydrochloric and sulphuric acid,<sup>31,38,39</sup> producing less than 100 nm in diameter. However, higher concentrations or temperatures of the acid mixture during hydrolysis led to the formation of nanocrystals instead of nanofibers.<sup>40</sup> Besides, the presence of sulfate groups from sulfuric acid hydrolysis reduced the thermal stability of the nanofiber.<sup>41</sup>

Appropriate pretreatments of cellulose fibers before or after sonication were reported to increase fiber reactivity and simplify the extraction.<sup>42</sup> Another chemical pretreatment recently reported to exhibit a promising method of breaking down cellulose fibers prior to mechanical fibrillation is carboxymethylation.<sup>43</sup> Carboxymethylation pretreatment onto cellulosic fiber is done by replacing hydroxyl groups with

carboxymethyl groups in an alkaline medium. It was reported that the presence of carboxymethyl groups resulted in a lower number of passes during mechanical fibrillation due to the increase of electrostatic repulsion between the fibrils.<sup>44</sup> The strength of hydrogen bonding and hydrophobic nature within the cellulosic fibers was reduced with the addition of charged groups,<sup>27</sup> leading to ease in the subsequent fibrillation. Even though carboxymethylation pretreatment prior to mechanical fibrillation was identified as causing constraints, such as excessive depolymerization and the existence of negatively-charged surfaces,<sup>45</sup> a significant reduction in energy used during the manufacturing of the carboxymethyl cellulose could compensate for these drawbacks.<sup>46</sup> Besides, from viewpoint of producing cellulose microfibrils, negatively-charged surfaces did not affect the morphological dimension of individual fibrils.<sup>44</sup> For this, the study is attributed to the isolation technique through chemical pretreatment to encourage the production of this renewable material for new uses, in line with the current production method of micro- and nanofiber.

According to the literature, the isolation of cellulose microfibrils from oil palm frond (OPF), using ultrasonication with the help of carboxymethylation pretreatment, remains unexplored. Thus, our research focuses on carboxymethylation as a chemical pretreatment approach that may be used in conjunction with ultrasonication as a mechanical fibrillation technique to produce micro-sized cellulose fibers. Since the properties of fibrils are greatly influenced by the raw materials used and their preparation (including fibrillation), the morphological and thermal behavior of microfibrils isolated using the carboxymethylation pretreatment strategies prior to the ultrasonication fibrillation is the main focus of this paper. Their morphological and thermal properties are compared with microfibers isolated using other physical pretreatment methods, such as high-speed blending, high-shear homogenization and simple magnetic stirring. The width distribution of the cellulose microfibrils produced is investigated using field emission scanning electron microscopy (FESEM), and the thermal behavior was evaluated from thermogravimetric analysis (TGA). The morphological behavior of the fibrils was later confirmed using X-ray diffraction (XRD) analysis. The findings presented in this study are

expected to facilitate the potential of combining pretreatment with ultrasonication to convert one of the oil palm wastes into a value-added component, with the intention of cleaner waste management from the oil palm industry and, as a result, a lower environmental impact in the future.

## EXPERIMENTAL

### Pretreatment of OPF cellulose fiber

The bleached cellulose utilized in this investigation was extracted from OPF using the procedure described by Kumneadklang *et al.* with some modifications.<sup>47</sup> The oil palm fronds (OPF) fiber was directly treated with 8 wt% NaOH at 90-100 °C for 2 hours using a fiber-to-solution ratio of 1:20 by weight. The obtained black slurry from the alkaline treatment was filtered and the solid residue was washed with distilled water several times. The washing and filtering steps were repeated until the pH of the filtrate was neutral. The residue was then dried in the oven at 65 °C to constant weight for 24 hours. At this stage, oil palm frond cellulose was obtained. The OPF cellulose fiber was bleached with 30% H<sub>2</sub>O<sub>2</sub> at 90 °C for an hour, using a fiber to solution ratio of 1:20. The bleaching step was repeated three times until the cellulose turned white. After the white fiber solution was allowed to cool, it was rewashed using distilled water and finally dried in the oven at 65 °C for 24 hours.

The extracted cellulose fibers (OPF-C) were used in some parts of the analysis for comparison purposes. Monochloroacetic acid (ClCH<sub>2</sub>COOH), isopropanol (C<sub>3</sub>H<sub>8</sub>O), acetic acid (CH<sub>3</sub>COOH), methanol (CH<sub>3</sub>OH) and ethanol (C<sub>2</sub>H<sub>5</sub>OH) – used for the carboxymethylation pretreatment – were purchased from Sigma-Aldrich and used as received. All other chemicals were of analytical grade. Deionized (DI) water was utilized for all experiments.

### Carboxymethylation

Five grams of bleached cellulose fiber, OPF-C, was soaked in 100 mL of isopropanol and 20 mL of 52% (w/v) NaOH was added dropwise into the mixture. Isopropanol was used in alkalization as a solvent, and the fiber was left to soak for 60 min at 30 °C. Next, 10 g of monochloroacetic acid was added and kept at 55 °C under constant stirring conditions for 180 min using a water bath shaker. The slurry was filtrated, and the solid residue was soaked in methanol overnight to remove impurities. The suspension was then neutralized with 90% acetic acid. Finally, the solid residue was washed with ethanol, and the obtained carboxymethylcellulose was dried using a freeze dryer for 48 hours at -82 °C temperature. This procedure of carboxymethylation of OPF-cellulose fiber was adapted from the optimization study reported by Tasaso P. (2014)<sup>48</sup> with some minor modifications.

**High-shear homogenization**

High-shear homogenization was performed using an Ultra-Turrax T25 (I.K.A., Germany) homogenizer. An aqueous suspension with 0.2% (w/v) of bleached cellulose was prepared using 0.6 g of cellulose fiber extracted from oil palm frond in deionized water. The suspension was homogenized at 15,000 rpm for 10 min. The suspension was later subjected to fibrillation using ultrasonication.

**High-speed blending**

An aqueous suspension with 0.2% (w/v) of bleached cellulose was prepared by dispersing cellulose fiber extracted from oil palm frond in deionized water. The suspension was fibrillated using a high-shear ultrafine grinder at 15,000 rpm for 10 min. The suspension was later subjected to fibrillation using ultrasonication.

**Magnetic stirring**

The suspension of bleached cellulose extracted from oil palm frond was prepared at a weight-to-volume ratio of 0.2% (w/v) before the suspension was

allowed to be soaked under magnetic stirring at 450 rpm. After the suspension was stirred for 24 hours, the cellulose fiber was sonicated, as detailed in the next section.

**Isolation of cellulose microfibrils**

A 20 kHz ultrasonic processor (220V, Cole-Parmer, US), with a stainless 6-mm diameter probe, was used for the fibrillation of the pretreated cellulose suspension. The amplitude of the sonicator was set at 60%, and all the samples from various pretreatment steps were ultrasonicated for 30 min. The probe was ensured to remain well dipped into the cellulose suspension throughout the procedure. The temperature of the suspension was kept consistent by keeping the water flow through a double-wall beaker to remove any excess heat. Finally, all the samples were slowly frozen in a freezer (-2 °C) for 24 h, followed by lyophilizing in a vacuum freeze-drier (Labconco, US) at -82 °C at a pressure of 0.09 mbar for two days to remove water for further analysis. The summary of the fibrillation method is shown in a schematic diagram in Figure 1, and the notation is summarized in Table 1.

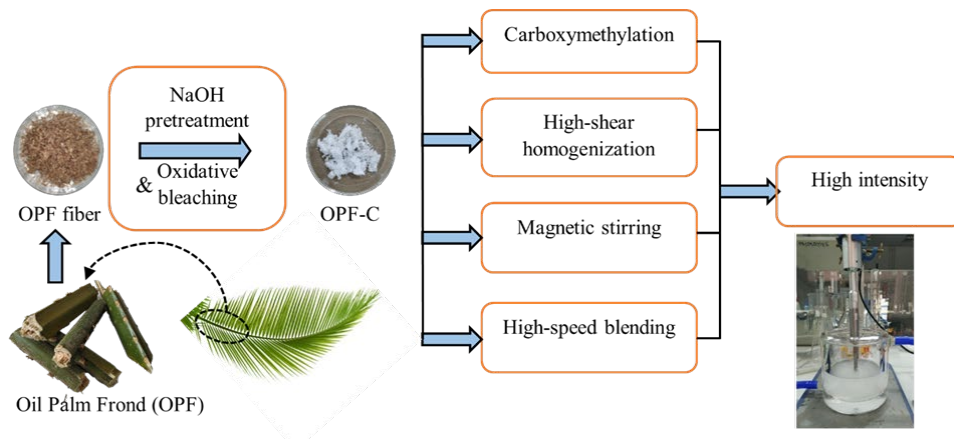


Figure 1: Schematic representation of pretreatment procedures applied on bleached OPF cellulose prior to high-intensity ultrasonication

Table 1  
Combination of pretreatment strategies and HIUS fibrillation method

Pretreatment strategy	Ultrasonication parameters	Sample
Carboxymethylation at 55 °C	30 min at 60% amplitude	CMF-CM
High-shear homogenization at 15,000 rpm for 10 min	30 min at 60% amplitude	CMF-HG
High-speed blending at 15,000 rpm for 10 min	30 min at 60% amplitude	CMF-HS
Magnetic stirring at 3000 rpm for 24 h	30 min at 60% amplitude	CMF-ST

**Characterization****Morphology**

The surface morphology and structures of raw OPF and extracted cellulose (OPF-C) were studied using scanning electron microscopy (SEM). The samples were first coated with gold by using a sputter coater device from Bal-Tec (Multi Coating System MED20); later, SEM (JEOL-JSM-6010LA) was applied at an

acceleration voltage of 15 kV. Meanwhile, the morphological studies of isolated cellulose microfibrils extracted from OPF that were pretreated using various methods were carried out using a field emission scanning electron microscope, FE-SEM (ZEISS-SUPRA 55VP), for higher resolution images. The freeze-dried samples were coated with gold using a sputter coater device. Then, the images were taken

using a secondary electron detector at 15 kV accelerating voltage.

#### **Thermogravimetric analysis/Differential thermal analysis (TGA/DT)**

The thermal behavior of raw dried oil palm frond fiber (OPF), the cellulose extracted (OPF-C), and commercial crystalline cellulose (Commercial) samples were investigated using a simultaneous thermal analyzer (Netzsch STA 449F3). Samples of CMF-CM, CMF-HG, CMF-HS and CMF-ST were also tested for their thermal stability. All the samples were heated from ambient temperature up to 800 °C under a nitrogen gas atmospheric condition. The heating rate was maintained at 10 °C/min. The weight of all tested samples was 5-7 mg. In addition, the energy requirement for thermal degradation of the extracted cellulose sample from OPF and CMF-CM sample were observed using DSC, with a heating rate of 10 °C/min under nitrogen flux.

#### **X-ray diffraction (XRD)**

The effect of pretreatments and mechanical fibrillation on the microfibrillated cellulose was also investigated using crystallinity index measurements taken from X-ray diffractograms (Bruker AXS-D8 Advance). The diffraction patterns of the freeze-dried samples were recorded using Cu radiation at 40 kV and 40 mA, with a Cu Ka X-ray source with the wavelength ( $\lambda$ ) of 0.15406 nm. The scans were performed from 5° to 60° with 0.05° increments. Cellulose crystallinities were determined using the deconvolution method.<sup>48</sup> The deconvolution of the X-ray diffraction patterns was performed with ORIGIN software to separate amorphous and crystalline contributions to the diffraction spectrum, using a curve-fitting process, in which the Gaussian function is used for the deconvolution of all the crystalline peaks. The crystallinity index,  $C_I$ , of the microfibril samples was calculated using Equation 1 below:

$$C_I(\%) = \left( \frac{A_c}{A_t} \right) \times 100 \quad (1)$$

where  $A_c$  is the integrated area of crystalline peaks in the X-ray diffraction and  $A_t$  is the total area under the X-ray diffraction curve. The average crystallite size was determined using the Scherrer equation, and the width of the diffraction patterns recorded in the X-ray reflected the crystalline area for both cellulose I and cellulose II crystals. It was determined using the following Equation 2:

$$D(\text{nm}) = \frac{k \lambda}{\beta \cos \theta} \quad (2)$$

where  $D$  is the crystallite size,  $k$  is the Scherrer constant (0.84),  $\lambda$  is the wavelength of the X-ray diffraction,  $\beta$  is the full-width at half (FWH) of the crystalline peaks (in radians) and  $\theta$  – the corresponding Bragg angle.

#### **Fourier transform infrared spectroscopy (FTIR)**

FTIR spectroscopy was utilized to identify potential changes in the functional groups in carboxymethylated cellulose, prior to the mechanical microfibrillation, compared with the extracted cellulose sample. FTIR spectra for the dried extracted cellulose (OPF-C) and CMF-CM sample were recorded using a Bruker Tensor 27 spectrometer (Bruker, Karlsruhe), equipped with a single reflection attenuated total reflectance (ATR) system. Bands were recorded in the region from 4000  $\text{cm}^{-1}$  to 600  $\text{cm}^{-1}$  at ambient temperature. The surface chemistry of the CMF-CM sample was discussed in the Results and Discussion section.

#### **Carboxyl group content**

The carboxyl group content of the prepared CMF-CM carboxymethylated pulp was determined using the conductometric titration method in accordance with SCAN-CM 65:02. Briefly, 1 g of oven-dried CMF-CM was converted to the proton form by dispersing in 0.1 M HCl and allowed to stand for 15 min, before being washed until the conductivity was less than 5  $\mu\text{S}/\text{cm}$ . Then, 490 mL of deionized water and 10 mL of 0.05 M NaCl were added and subsequently stirred thoroughly using a magnetic stirrer. The suspension was titrated against 0.05 M NaOH from a precision burette, and the titration was immediately stopped when the conductivity started to increase. The total amount of the carboxyl group present in the CMF-CM was calculated according to the following Equation 3:

$$\text{Carboxyl group content} = (C_{\text{NaOH}} \times V_{\text{NaOH}}) / w \quad (3)$$

where  $C_{\text{NaOH}}$ ,  $V_{\text{NaOH}}$ , and  $w$  are the concentration of the NaOH solution, the volume of the NaOH solution, and the oven-dry weight of the sample, respectively.

#### **Statistical analysis of diameter distributions**

The comparison of the pretreatment strategies used in this study was evaluated through the reliability of the morphological data collected from the FESEM analysis. The coefficient of variation (CV) onto the width (diameter) dispersion measurements were calculated for each of the pretreatment strategies, at which mean values and standard deviations of fiber width were first determined. CV was calculated as a ratio between the standard deviation and the mean of the distribution of the morphological data set. It is an estimate of the experimental error in relation to the overall average of the experiments with respect to the morphological results.

## **RESULTS AND DISCUSSION**

### **Morphological studies**

Kumneadklang *et al.* reported the main composition of raw oil palm frond consists of 42.67% cellulose, 34% hemicelluloses and 22.9% lignin.<sup>47</sup> The presence of these components will dramatically change as the fiber is subjected to

cellulose extraction procedures. They also reported that the cellulose content in the OPF increased up to 79.6% as the OPF was treated with an alkaline solution at a high temperature. This apparent composition change will affect its morphological and thermal characteristics. In this study, the cellulose extracted from OPF was subjected to carboxymethylation pretreatment and ultrasonication fibrillation to produce microfibrils. The SEM image of cellulose fiber before undergoing the carboxymethylation pretreatment and ultrasonication presented in Figure 2 shows a large bundle of fibers (diameter: 30–300  $\mu\text{m}$ ). The sequential processes have broken down the lignocellulosic complex, dissolved the lignin and hemicelluloses, and opened up the cellulose to allow extensive fibrillation in the subsequent process.

The field emission scanning electron micrograph images of the cellulose microfibrils isolated using carboxymethylation pretreatment methods are presented in Figure 3a. The micrographs of the microfibrils isolated using other pretreatment methods were also presented in Figure 3b-d. From the FESEM image of the microfiber, the morphological structure of the OPF cellulose fiber differs significantly from that of the cellulose microfibrils after undergoing ultrasonication fibrillation. Various pretreatment strategies and the 30-min ultrasonication method have caused a significant reduction in cellulose fiber dimensions, causing the bundles to separate into individual microfibrils. The diameter of the microfibrils was measured using ImageJ software, and the frequency distribution was plotted to study the significance of pretreatment strategies

prior to the ultrasonication by assuming their cross-section are circular.

By comparing the diameter distribution of cellulose microfibrils in Figure 3, carboxymethylation pretreatment has shown some extent of microfibrillation. Such a method has yielded individualized microfibrils down to an average width of 3.8  $\mu\text{m}$ . The addition of negatively charged groups (during carboxymethylation) to cellulosic fiber has improved fibril delamination and enabled the fibrillation of fibers with narrow-width distributions. It was reported that pretreatment with carboxymethylation induces electrostatic repulsion between fibers, allowing fibers to disintegrate into thinner fibrils.<sup>49</sup> The presence of the carboxyl group in the cellulose fiber wall has resulted in lower delamination resistance and hence eases further fibrillation.<sup>27</sup> The addition of  $\text{Na}^+$  ions during carboxymethylation disrupts the cellulose hydrogen-bonded crystalline region (internal fibrillation),<sup>50</sup> thus weakening the bond that exists inside the fiber and when the external fibrillation is applied via hydrodynamic forces (HIUS), the fiber breaks into micron-sized fibers.

The average diameter of cellulose microfibrils isolated using a combination of high-shear homogenization and HIUS is 7.8  $\mu\text{m}$ , slightly smaller than microfibrils isolated using the combination of high-speed blending and magnetic stirring, which are measured at 9.4 and 9.5  $\mu\text{m}$ , respectively. The width distribution for the later pretreatment strategies spans out at wider distribution up to 30  $\mu\text{m}$ , showing some fiber fragments and bundles are still inhomogeneous in size.

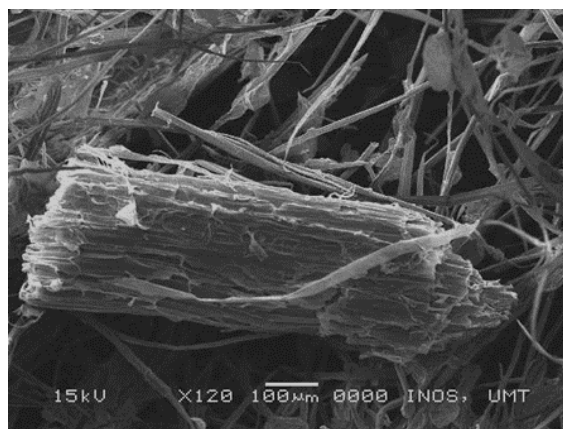


Figure 2: SEM image of cellulose extracted from oil palm frond showing large size of the fiber bundle

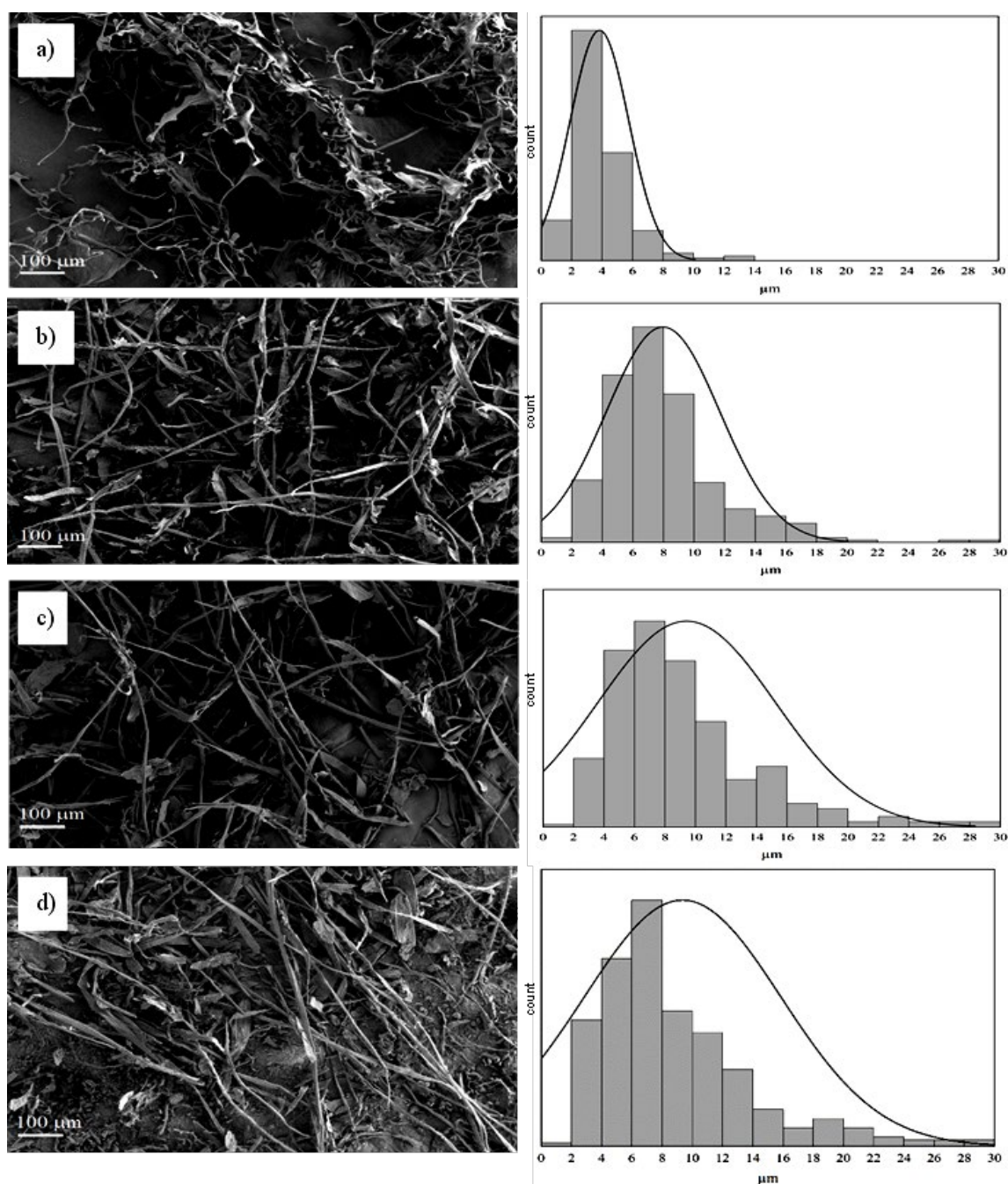


Figure 3: Field-emission scanning electron micrographs of microfibrillated cellulose isolated using high-intensity ultrasonication with various pretreatment: a) carboxymethylation (CMF-CM), b) homogenization (CMF-HG), c) high-speed blending (CMF-HS), d) magnetic stirring (CMF-ST) and their corresponding diameter size distribution

A more homogenous structure is seen for microfibrils isolated using carboxymethylation pretreatment, as shown in Figure 3a. When subjected to ultrasonic treatment operating at atmospheric pressure, the cellulose fibers treated with pre-mechanical strategies, such as high-shear homogenizer, high-speed blending, and stirring, are exposed to oscillating power, which creates hydrodynamic forces that are effective in

consolidating them into the micron-long fibrils.<sup>51</sup> The mechanical oscillating power applied in liquid with suspended fiber leads to the formation, expansion, and implosion of microscopic gas,<sup>52</sup> in which a violent shock wave applied on the surfaces of the fibers has created external fibrillation that causes breakage of intermolecular hydrogen bonding in cellulose.

The significance of pretreatment strategies in producing microfiber from OPF-based cellulose could be contemplated statistically. The statistical measure of reliability distribution of the data set for microfiber width for all types of pretreatment was evaluated based on the coefficients of variation value. CV is calculated as the ratio between the standard deviation and the mean values in the diameter size distribution data measured from FESEM images using ImageJ software. The number of data (counts) for measured fiber used to evaluate the CV value is approximately the same to ensure the consistency of the results. The CV value analyzed is tabulated in Table 2. A larger value of CV reflects the

variability of diameter values from its mean value, representing the more spread of the fiber diameter around its mean. The CV value for microfiber isolated using carboxymethylation pretreatment combined with ultrasonication (CMF-CM) showed the lowest value at 44.4%, representing the lowest variability of the diameter data. It demonstrates the method used to isolate the microfiber for this type of sample is statistically reliable and corresponds to the greater quality of the experimental method.<sup>53</sup> It is supported by a small standard error value, which reflects a good representation of the measured sample compared to the overall data.

Table 2  
Statistical parameters on the measurement of microfiber diameter measured from FESEM images

Sample	Counts	Standard error	CV (%)
CMF-CM	352	0.09	44.4
CMF-HG	313	0.21	46.6
CMF-HS	336	0.35	69.5
CMF-ST	348	0.31	61.7

### Crystallinity index studies

The XRD analysis of the cellulose extracted from OPF (OPF-C) and cellulose microfibrils was used to determine the changes in crystalline structure as the extracted cellulose from oil palm fronds was subjected to various pretreatment techniques and ultrasonication procedures. The crystallinity index is one of the significant aspects of the cellulose microfibrils fiber in ascertaining its thermal and mechanical stability. Figure 4 depicts the overlay of the X-ray diffraction patterns for all cellulose microfibrils isolated using different pretreatment strategies prior to the ultrasonication process, compared to the diffraction pattern for extracted cellulose, OPF-C.

It can be observed that the OPF-C, CMF-HG, CMF-HS and CMF-ST samples exhibit the characteristic peaks at  $2\theta=22^\circ$  and  $16^\circ$ , which are ascribed to the (002) and (101) crystallographic planes of the typical structure of cellulose I.<sup>54</sup> The diffraction peaks observed within the mentioned range depict the diffraction intensity of crystalline regions (regarded as primary peak) and amorphous (secondary peak), respectively. These observations indicate that the crystalline structure of cellulose I remains intact despite the consecutive mechanical pretreatment and high-intensity ultrasonication process. The cellulose microfibrils isolated using pre-mechanical

strategies exhibit more intense diffraction at the primary peak than their origin (OPF-C) sample, implying a higher degree of crystallinity. It is attributed to the elimination of certain amorphous components and the reorganization of the crystalline regions into a more ordered structure<sup>55</sup> during the pretreatment process. These trends were consistent with the morphology in FESEM images (Fig. 3) of the microfibrils, showing more crystalline structure as compared to OPF-C (SEM image in Fig. 2).

In contrast, the cellulose microfibrils isolated using carboxymethylation pretreatment with a combination of ultrasonication shearing, CMF-CM, has shown a different diffraction pattern in terms of heights, peak shifts, and peak widths. Typical crystalline peaks of cellulose I structure at diffraction angles of  $2\theta = 22^\circ$  and  $16^\circ$  observed in OPF-C samples disappeared for CMF-CM samples. Instead, a strong diffraction peak at  $2\theta = 20^\circ$  was observed. The observation indicates that the carboxymethylation process has disrupted the cellulose crystalline structure and feasibly caused the structure to shift from cellulose I to cellulose II.<sup>56</sup> The occurrence may be due to the cleavage of the hydrogen bonds, as carboxymethyl groups substituted the hydroxyl groups in the OPF-C. The shifting of the peaks was attributed to the destruction of  $\beta$ -glycosidic linkage, which

increased the distance between cellulose molecules.<sup>57</sup> The combination of carboxymethylation and HIUS fibrillation also led to a 21% decrease in the crystallinity index of CMF-CM, compared with the extracted cellulose. Onyianta *et al.* have reported a 35% decrease in crystallinity index for the cellulose nanofiber isolated from the commercial hardwood bleached

cellulose sample after it underwent carboxymethylation and subsequent mechanical homogenization.<sup>27</sup> Im *et al.* also reported the same observation for the carboxymethylation treatment applied to eucalyptus kraft pulp in the production of cellulose nanofibrils.<sup>44</sup> The crystallinity indexes of the different samples are given in Table 3.

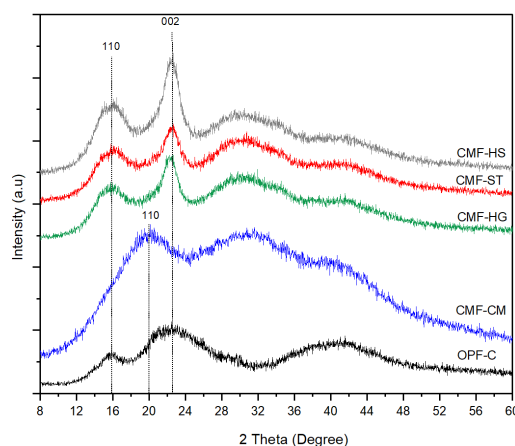


Figure 4: Overlay XRD patterns within  $2\theta$  scale ranging from  $5^\circ$  to  $60^\circ$  of the cellulose microfibrils isolated using the combination of various pretreatment and ultrasonic shear as compared to extracted cellulose from oil palm frond biomass, OPF-C.

Table 3  
Crystallinity indices of extracted cellulose and microfibril samples from OPF

Sample	Crystallinity index, CrI (%)	Average crystallite size (nm)
OPF-C	31.78	6.653
CMF-CM	25.11	2.421
CMF-HG	35.59	4.205
CMF-HS	32.62	3.301
CMF-ST	33.56	3.605

### Thermal analysis

The thermal properties of cellulose microfibrils are an essential factor in evaluating their applicability as solar thermal insulation materials. The TGA thermogram for microfibrils isolated through different pretreatment strategies is shown in Figure 5. The thermogram shows the initial weight loss observed in all cellulose microfibril samples within the range of 35-150 °C, representing the evaporation of the loosely bound moisture on the surface of these materials. The TGA images of the microfibrils isolated from OPF-C, using the combination of carboxymethylation (chemical) and ultrasonication (physical) technique, showed a quite significant mass loss at approximately 220 °C, while the microfibrils isolated from the same source using the combination of pre-mechanical

strategies have retained their thermal integrity up to the same temperature. This can be seen from the TGA curves for CMF-HG, CMF-HS and CMF-HS, which degrade at a temperature higher than 250 °C, with a significant weight loss exceeding 50% for all the samples.

Derivative thermogravimetric analysis (DTG) for all CMF samples was plotted from 25 °C to 1000 °C to analyze the stages of degradation further. The DTG diagram in Figure 6 shows that CMF-CM microfibre degraded in three phases; however, CMF-HG, CMF-HS, and CMF-ST degraded in two stages over the indicated range. The first stage of degradation started at room temperature up to 200 °C, representing the vaporization of water molecules in the fibers. This stage of degradation is relatively high for microfibre pretreated by carboxymethylation

(CMF-CM), which accounts for 15.76% of its mass change. This observation could be explained by the substitution of some parts of hydroxyl groups in the cellulose fiber with the hydrophilic

carboxymethyl groups,  $\text{CH}_2\text{COONa}$ , which hence increased the absorption of more water molecules,<sup>58</sup> as compared to the other three samples.

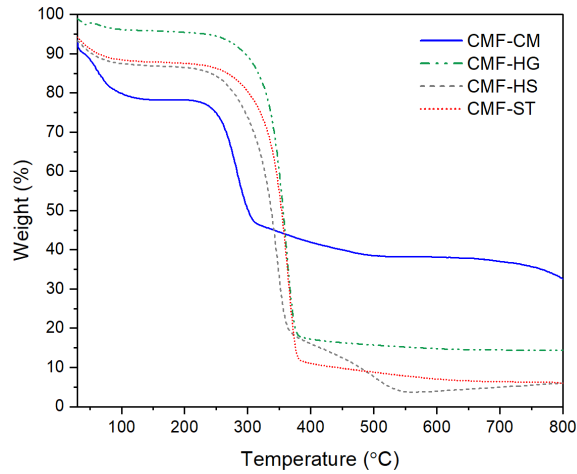


Figure 5: Thermogram profile of cellulose microfibrils isolated using the combination of various pretreatment and high-intensity ultrasonication (HIUS)

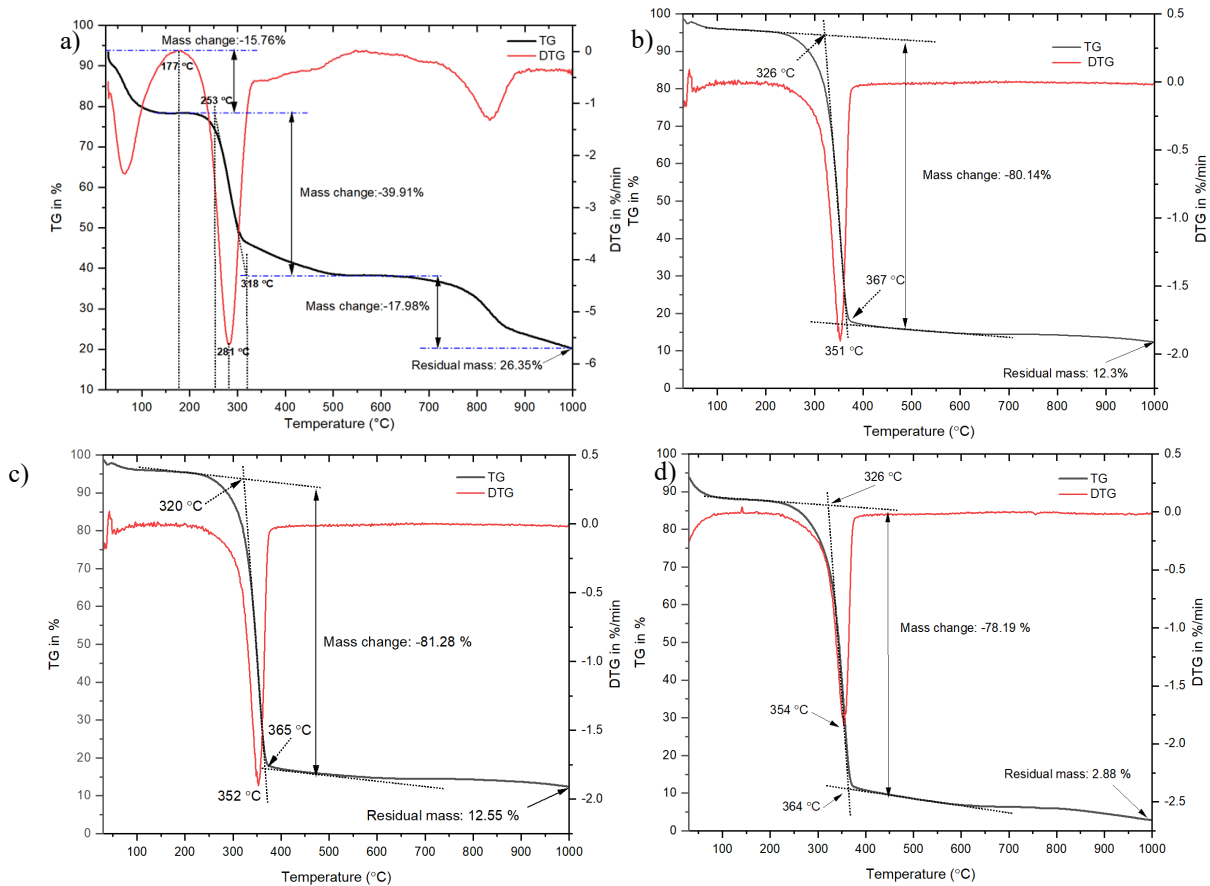


Figure 6: Derivative thermogravimetric (DTG) diagrams of microfibrils: (a) CMF-CM, (b) CMF-HG, (c) CMF-HS and (d) CMF-ST

A dramatic mass loss shown in the second stage of degradation for all samples was attributed to the depolymerization of carbohydrates and

lignin. Apart from depolymerization, the second stage of degradation is also caused by decarboxylation,<sup>59</sup> the rearrangement of carboxyl

groups and eventually results in the unfolding of carbon dioxide and carbon monoxide. The second thermal degradation for CMF-CM was observed to start at 177 °C, which is lower than for other microfibrils. The thermal degradation of the second phase in the fiber accounts for major mass loss (39.91%), which is associated with the amorphous structure developed during carboxymethylation pretreatment and could cause the CMF-CM sample to degrade at a lower temperature than in the case of microfibrils pretreated with mechanical treatment. The lower thermal stability of CMF-CM, as compared to other cellulose microfibrils, is consistent with its crystallinity index explained in the previous section. This is due to the fact that an amorphous structure starts to degrade at a lower temperature, as compared to a crystalline structure.<sup>60</sup> Compared to other types of cellulose microfibrils, the lower thermal stability of CMF-CM could also be attributed to the presence of sodium carboxylates on the surface of CMF-CM.<sup>27</sup> This reduction might also correspond to the high surface area of microfibrils in the CMF-CM (small average diameter), which accelerates the heat transfer rate and consequently lowers the decomposition temperature.<sup>52,61</sup>

A sharp peak for the second stage of degradation represents the maximum degradation rate temperature ( $T_{max}$ ) recorded at 281 °C (peak temperature) for CMF-CM, which is attributed to the degradation of the cellulose constituent. It is worth noting that the CMF-HG, CMF-HS, and CMF-ST samples all have a maximum temperature higher than 350 °C. This observation may be because the carboxymethylation pretreatment initiates more active sites and accelerates the decomposition. The  $T_{max}$  value recorded for CMF-CM is relatively lower than that for the microcrystalline cellulose (MCC) extracted from OPF by acid hydrolysis using hydrochloric acid, which was recorded at 345

°C,<sup>62</sup> but comparable with those for other cellulose microfibrils extracted from different types of biomass, such as oil palm mesocarp (240 °C),<sup>63</sup> sunflower stalk (295 °C),<sup>64</sup> oil palm empty fruit bunch (326 °C)<sup>65</sup> and coconut empty fruit bunch (325 °C).<sup>66</sup> The sample showed a quite significant mass loss from the temperature range of 606 °C and 1000 °C (in the third stage) attributed to the oxidative degradation of residue, leaving a residual mass of 26.35%. This fiber residue indicates the presence of carbonaceous materials in the nitrogen atmosphere. The comparison of the thermal characteristic of all samples is tabulated in Table 4.

The energy consumption property of CMF-CM during the thermal degradation was also analyzed with respect to the extracted cellulose sample (OPF-C) using differential scanning calorimetry. Differential scanning calorimetry, or DSC, is an analytical technique that can determine the amount of energy needed for the thermal destruction of inorganic and organic substances. Figure 7 shows the differential scanning calorimetric curves of CMF-CM and its original cellulosic fiber extracted from the oil palm frond. Initial endothermic peaks in DSC are due to the bound water molecules in the fibers. The presence of non-substituted hydroxyl groups in cellulose creates a strong affinity for water.<sup>67</sup> However, the presence of carboxyl groups in carboxymethylated cellulose creates a stronger affinity for water molecules than hydroxyl groups.<sup>68</sup> It can be seen from significant endothermic peaks in the DSC thermogram for the CMF-CM sample within the water evaporations range, indicating a strong water-holding capacity and water-polymer interaction. After carboxymethylation, the hydroxyl groups were replaced by carboxylate groups, capable of binding more water molecules by forming new hydrogen bonds, thus increasing the bound water content.

Table 4  
Comparison of thermal degradation characteristics of microfibrils isolated using different pretreatment

Samples	Onset temperature (°C)	2 <sup>nd</sup> Stage degradation peak temperature (°C)	Residual mass (%)
CMF-CM	253	281	26.35
CMF-HG	326	351	12.30
CMF-HS	320	352	12.55
CMF-ST	326	354	2.88

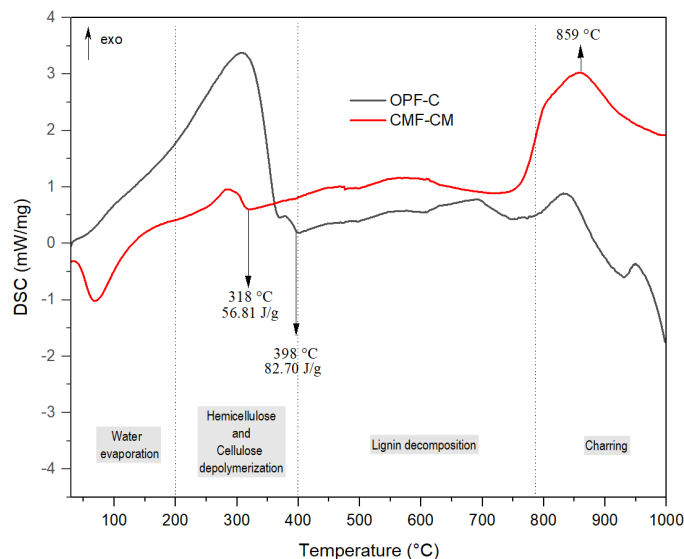


Figure 7: Differential scanning calorimetric curve of microfibrillated cellulose fiber treated using carboxymethylation and initial extracted cellulose fiber from OPF

The initial endothermic peak is also associated with the glass transition stage, where the amorphous components are converted from a brittle state to a rubbery state. The CMF-CM samples have more amorphous components than the originally extracted cellulose, thus showing a significant endotherm peak within this region. The second endothermic transition in the DSC thermogram within the temperature range of 250–400 °C corresponds to the crystalline part of the cellulosic fiber,<sup>69</sup> as the energy absorbed within this region corresponds to the breakage of the glycosidic bond in the cellulose. The second endothermic peak (melting temperature,  $T_m$ ) was recorded at 318 °C for CMF-CM, in agreement with the onset temperature and maximum mass change in the second stage of thermal degradation measured in the TG diagram. The melting temperature for extracted cellulose was a little higher, which is at 398 °C. This difference in melting temperature results from the changes in crystallinity due to the presence of relatively large groups of carboxymethyl, causing irregularities in the cellulose chain.<sup>70</sup> However, the melting temperature recorded for CMF-CM was relatively higher than for the microcrystalline cellulose extracted from OPF reported by Hussin *et al.*, which was recorded at 220 °C.<sup>71</sup> A recent study has demonstrated that carboxymethylation can significantly improve cellulose-based composite's thermal stability.<sup>72</sup> The endothermic peak for CMF-CM is comparable to that of cellulose extracted from other agricultural biomass sources like maize stalk (330 °C), soybean hull (314 °C)<sup>73</sup>

and sugarcane bagasse (339 °C).<sup>74</sup> Endothermic peaks observed at temperatures beyond 400 °C represent the energy required to decompose lignin and other non-cellulosic components. According to Yang *et al.*, lignin degradation slowly continues from 100 up to 900 °C.<sup>75</sup> The decomposition of lignin and other non-cellulosic components in the CMF-CM continues up to 730 °C. The breakdown of functional groups in residues of carboxymethylated cellulose occurred at higher temperatures, and the heat released signifying a charring process, giving the exothermic peak that can be observed at 859 °C, correlated with the third stage of significant mass loss recorded in the TG diagram.

### Surface chemistry analysis of CMF-CM

The changes in the properties in the extracted cellulose sample due to the carboxymethylation pretreatment prior to the ultrasonication fibrillation could be explained by the functional groups present in the sample, evaluated from the FTIR analysis. OPF lignocellulosic fiber consists of three primary components (*i.e.*, lignin, hemicelluloses and cellulose). These materials comprise various oxygen-containing functional groups like alcohols, alkanes, aromatics, esters, and ketones.<sup>76</sup> The FTIR spectra were scrutinized within the range of 600  $\text{cm}^{-1}$  and 4000  $\text{cm}^{-1}$  for extracted cellulose and CMF-CM samples, as shown in Figure 8.

Both OPF-C and CMF-CM samples exhibited quite similar and dominant peaks in the absorbance region between 3600  $\text{cm}^{-1}$  and 2500

$\text{cm}^{-1}$ . The first peak was observed at  $3300 \text{ cm}^{-1}$ , attributed to O–H stretching vibration, representing intramolecular hydrogen bonds and hydroxyl groups in the cellulose structure.<sup>77</sup> However, the chemical pretreatment (carboxymethylation) has changed the intensity of the peak in CMF-CM, indicating a change in the intensity of hydroxyl groups in the CMF-CM sample. The second significant peak was observed around  $2900 \text{ cm}^{-1}$ , which is associated with asymmetric stretching vibrations of C–H.<sup>78</sup> Therefore, the peak could signify that both samples were composed mainly of alkyl and

aliphatic compounds, abundantly found in cellulose.<sup>79</sup>

The FTIR spectrum of the CMF-CM sample exhibited a strong absorption at  $1605 \text{ cm}^{-1}$ , as compared to that of extracted cellulose, indicating the presence of a carboxymethyl constituent in the sample.<sup>80</sup> Hutomo *et al.* also reported that the wavenumber  $1604 \text{ cm}^{-1}$  corresponds to the C=O group stretching of carboxymethyl functional groups.<sup>81</sup> The absorption peak at  $1420 \text{ cm}^{-1}$  confirms the presence of strong hydrophilic carboxylate groups.

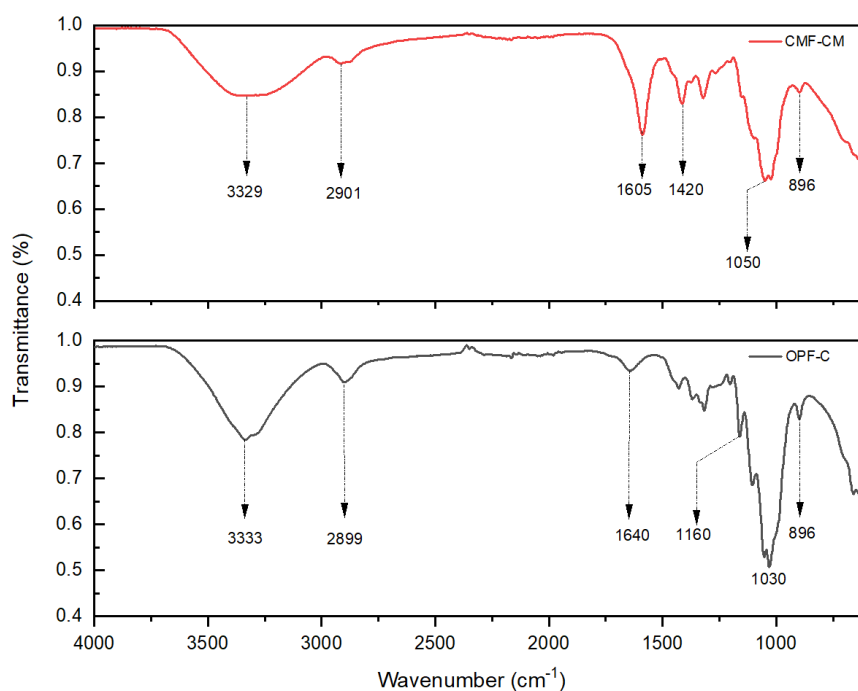


Figure 8: Comparison of FTIR spectra of extracted cellulose (OPF-C) and CMF-CM sample

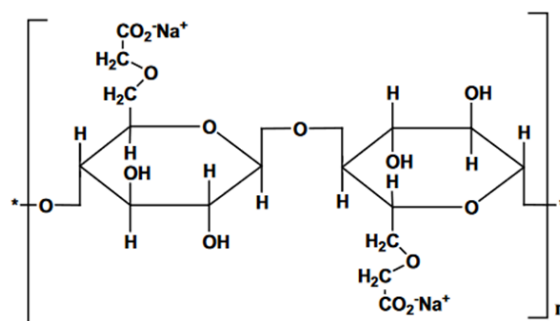


Figure 9: Molecular structure of carboxymethylated cellulose<sup>85</sup>

The reduction in the absorption peak area associated with –OH stretching vibration ( $3300 \text{ cm}^{-1}$ ) in the CMF-CM sample (as compared to its origin extracted cellulose sample) and the increase in peak intensity of the absorption peaks

at  $1605 \text{ cm}^{-1}$  and  $1420 \text{ cm}^{-1}$  explain the reduction in the –OH groups as due to the attachment of the carboxylate groups, as illustrated in the carboxymethylated cellulose chemical structure in Figure 9. The calculated carboxyl group content

for CMF-CM prepared was 470  $\mu\text{mol/g}$ . This value is relatively low, compared to the value reported in the literature, which is between values of 515–610  $\mu\text{mol/g}$ .<sup>27,83</sup>

On a different note, the peak absorbed at 1640  $\text{cm}^{-1}$  in the extracted cellulose is attributed to the H–O–H stretching vibration of absorbed water in carbohydrates.<sup>62,84</sup> The reaction of alkaline during the extraction with –OH groups from the cellulose in the samples and the subsequent formation of water molecules contribute to this peak in the spectra.<sup>79,85</sup> Even though the samples were dried during the extraction process, the water adsorbed in the cellulose molecules remained due to natural cellulose–water interactions.<sup>79</sup>

It is worth noting the absorbance peak within the fingerprint region as it is typically specific and unique. The fingerprint region lies within the range of 600–1500  $\text{cm}^{-1}$  in the FTIR spectra. For the lignocellulosic sample, the absorbance peak between 1160 and 890  $\text{cm}^{-1}$  represents the typical cellulose characteristics.<sup>86</sup> The significant peak observed at 1160, 1050, and 1030  $\text{cm}^{-1}$  for both OPF-C and CMF-CM samples is due to the C–O–C pyranose ring (antisymmetric in phase ring) in the cellulose.<sup>87</sup> All the samples also show a significant peak at 896  $\text{cm}^{-1}$ , attributed to the  $\beta$ -glycosidic linkage, a unique feature of the cellulose structure.<sup>88</sup>

## CONCLUSION

Morphological and thermal properties of microfibrillated cellulose isolated using the combination of carboxymethylation pretreatment and high-intensity ultrasonication have been investigated and compared with those of microfibrils pretreated with other low-cost ambient pressure pretreatment strategies. Morphological observations of the microfibers revealed that carboxymethylation and ultrasonication could ease the fibrillation process, leading to cellulose microfiber of 3.8–10  $\mu\text{m}$  in diameter, with a high aspect ratio. High-shear homogenization and high-speed blending pretreatment also produced a bit larger microfibrils, yet with an average diameter lower than 10  $\mu\text{m}$ . The crystallinity index indicated the chemical pretreatment had changed the crystalline structure of microfibrillated cellulose into a more amorphous arrangement, at which the crystallinity index of CMF-CM has reduced, as compared to the initial extracted cellulose. The change in amorphous structure has affected the thermal degradation of carboxymethylated

cellulose. The presence of sodium carboxylates on the surface of CMF-CM caused its lower thermal stability, giving the peak degradation temperature at 281  $^{\circ}\text{C}$ , with the heat of fusion recorded at 56.81 J/g. The changes in crystallinity due to the presence of relatively large groups of carboxymethyl also reduced the melting temperature of CMF-CM, as compared to the initial extracted cellulose. The surface chemistry of CMF-CM confirms the presence of carboxylate ions in the sample. Statistical analysis of the variability value of morphological data using the coefficient of variation method validates the reliability of the carboxymethylation pretreatment strategy used in the study. The finding in this study corroborates the use of carboxymethylation pretreatment as an effective technique to aid the microfibrillation of cellulose from oil palm biomass, thereby could promise clean alternative waste management for the said industry. It also opens up more options for providing a viable supply of microfibrillated cellulose for solar thermal application in the future.

**ACKNOWLEDGMENTS:** Funding from the Fundamental Research Grant Scheme (FRGS/1/2019/TK10/UKM/02/1) by the Ministry of Higher Education is gratefully acknowledged for support in completing our original work. The authors thank the Research Laboratory of the University of Technology MARA, Bukit Besi Campus, for assisting with the research works.

## REFERENCES

- 1 S. B. Hansen, R. Padfield, K. Syayuti, S. Evers, Z. Zakariah *et al.*, *J. Clean. Prod.*, **100**, 140 (2015), <https://doi.org/10.1016/j.jclepro.2015.03.051>
- 2 J. A. Garcia-Nunez, N. E. Ramirez-Contreras, D. T. Rodriguez, E. Silva-Lora, C. S. Frear *et al.*, *Resour. Conserv. Recycl.*, **110**, 99 (2016), <https://doi.org/10.1016/j.resconrec.2016.03.022>
- 3 R. Uning, M. T. Latif, M. Othman, L. Juneng, N. M. Hanif *et al.*, *Sustainability*, **12**, 5077 (2020), <https://doi.org/10.3390/su12125077>
- 4 N. N. Ab. Rasid, A. Shamjuddin, A. Z. Abdul Rahman and N. A. S. Amin, *J. Clean. Prod.*, **321**, 129038 (2021), <https://doi.org/10.1016/j.jclepro.2021.129038>
- 5 J. C. Kurnia, S. V. Jangam, S. Akhtar, A. P. Sasmito and A. S. Mujumdar, *Biofuel Res. J.*, **3**, 332 (2016), <https://doi.org/10.18331/BRJ2016.3.1.3>
- 6 E. Onoja, S. Chandren, F. I. Abdul Razak, N. A. Mahat and R. A. Wahab, *Waste Biomass Valoriz.*, **10**, 2099 (2019), <https://doi.org/10.1007/s12649-018-0258-1>

- <sup>7</sup> S. K. Loh, S. James, M. Ngatiman, K. Y. Cheong, Y. M. Choo *et al.*, *Ind. Crop. Prod.*, **49**, 775 (2013), <https://doi.org/10.1016/j.indcrop.2013.06.016>
- <sup>8</sup> M. A. Nasution, T. Herawan and M. Rivani, *Energ. Proc.*, **47**, 166 (2014), <https://doi.org/10.1016/j.egypro.2014.01.210>
- <sup>9</sup> Q. Wu, T. C. Qiang, G. Zeng, H. Zhang, Y. Huang *et al.*, *Int. J. Hydrogen Energ.*, **42**, 23871 (2017), <https://doi.org/10.1016/j.ijhydene.2017.03.147>
- <sup>10</sup> S. S. Qureshi, S. Nizamuddin, H. A. Baloch, M. T. H. Siddiqui, N. M. Mubarak *et al.*, *Biomass Convers. Bioref.*, **9**, 827 (2019), <https://doi.org/10.1007/s13399-019-00381-w>
- <sup>11</sup> M. H. Hussin, A. A. Rahim, M. N. Mohamad Ibrahim and N. Brosse, *Ind. Crop. Prod.*, **49**, 23 (2013), <https://doi.org/10.1016/j.indcrop.2013.04.030>
- <sup>12</sup> A. E. Pirtsul, A. Krainov, M. I. Rubtsova, R. I. Mendgaziev, K. A. Cherednichenko *et al.*, *Mater. Lett.*, **308**, 131173 (2022), <https://doi.org/10.1016/j.matlet.2021.131173>
- <sup>13</sup> H. Zhong, Y. Li, P. Zhang, S. Gao, B. Liu *et al.*, *ACS Nano*, **15**, 10076 (2021), <https://doi.org/10.1021/acsnano.1c01814>
- <sup>14</sup> D. Yin, J. Mi, H. Zhou, X. Wang and H. Tian, *Carbohydr. Polym.*, **247**, 116708 (2020), <https://doi.org/10.1016/j.carbpol.2020.116708>
- <sup>15</sup> P. Gupta, B. Singh, A. K. Agrawal and P. K. Maji, *Mater. Des.*, **158**, 224 (2018), <https://doi.org/10.1016/j.matdes.2018.08.031>
- <sup>16</sup> F. Jiang, H. Liu, Y. Li, Y. Kuang, X. Xu *et al.*, *ACS Appl. Mater. Interfaces*, **10**, 1104 (2018), <https://doi.org/10.1021/acsnano.1c01814>
- <sup>17</sup> Y. Zhang, N. Hao, X. Lin and S. Nie, *Carbohydr. Polym.*, **234**, 115888 (2020), <https://doi.org/10.1016/j.carbpol.2020.115888>
- <sup>18</sup> S. Chen, G. Schueneman, R. B. Pipes, J. Youngblood and R. J. Moon, *Biomacromolecules*, **15**, 3827 (2014), <https://doi.org/10.1021/bm501161v>
- <sup>19</sup> N. Kawee, N. T. Lam and P. Sukyai, *Carbohydr. Polym.*, **179**, 394 (2018), <https://doi.org/10.1016/j.carbpol.2017.09.101>
- <sup>20</sup> D. Lin, R. Li, P. Lopez-Sanchez and Z. Li, *Food Hydrocoll.*, **44**, 435 (2015), <https://doi.org/10.1016/j.foodhyd.2014.10.019>
- <sup>21</sup> X. Hua, S. Xu, M. Wang, Y. Chen, H. Yang *et al.*, *Food Chem.*, **232**, 443 (2017), <https://doi.org/10.1016/j.foodchem.2017.04.003>
- <sup>22</sup> C. S. J. Chandra, N. George and S. K. Narayanankutty, *Carbohydr. Polym.*, **142**, 158 (2016), <https://doi.org/10.1016/j.carbpol.2016.01.015>
- <sup>23</sup> A. Tripathi, A. Ferrer, S. A. Khan and O. J. Rojas, *ACS Sustain. Chem. Eng.*, **5**, 2483 (2017), <https://doi.org/10.1021/acsschemeng.6b02838>
- <sup>24</sup> H. Taheri and P. Samyn, *Cellulose*, **23**, 1221 (2016), <https://doi.org/10.1007/s10570-016-0866-5>
- <sup>25</sup> S. S. Nair, J. Y. Zhu, Y. Deng and A. J. Ragauskas, *J. Nanopart. Res.*, **16**, 2349 (2014), <https://doi.org/10.1007/s11051-014-2349-7>
- <sup>26</sup> C. Hu, Y. Zhao, K. Li, J. Y. Zhu and R. Gleisner, *Holzforschung*, **69**, 993 (2015), <https://doi.org/10.1515/hf-2014-0219>
- <sup>27</sup> A. J. Onyianta, M. Dorris and R. L. Williams, *Cellulose*, **25**, 1047 (2018), <https://doi.org/10.1007/s10570-017-1631-0>
- <sup>28</sup> N. Lavoine, I. Desloges, A. Dufresne and J. Bras, *Carbohydr. Polym.*, **90**, 735 (2012), <https://doi.org/10.1016/j.carbpol.2012.05.026>
- <sup>29</sup> Z. Hu, R. Zhai, J. Li, Y. Zhang and J. Lin, *Int. J. Polym. Sci.*, **2017**, 1 (2017), <https://doi.org/10.1155/2017/9850814>
- <sup>30</sup> P. C. S. F. Tischer, M. R. Sierakowski, H. Westfahl and C. A. Tischer, *Biomacromolecules*, **11**, 1217 (2010), <https://doi.org/10.1021/bm901383a>
- <sup>31</sup> F. Fahma, S. Iwamoto, N. Hori, T. Iwata and A. Takemura, *Cellulose*, **17**, 977 (2010), <https://doi.org/10.1007/s10570-010-9436-4>
- <sup>32</sup> A. Isogai and L. Bergström, *Curr. Opin. Green Sustain. Chem.*, **12**, 15 (2018), <https://doi.org/10.1016/j.cogsc.2018.04.008>
- <sup>33</sup> D. Mishra, P. Khare, M. R. Das, S. Mohanty, D. U. Bawan Kule *et al.*, *Cellulose Chem. Technol.*, **52**, 9 (2018), [https://cellulosechemtechnol.ro/pdf/CCT1-2\(2018\)/p.9-17.pdf](https://cellulosechemtechnol.ro/pdf/CCT1-2(2018)/p.9-17.pdf)
- <sup>34</sup> M. Martelli-Tosi, M. D. S. Torricillas, M. A. Martins, O. B. G. D. Assis and D. R. Tapia-Blácido, *J. Nanomater.*, **2016**, 1 (2016), <https://doi.org/10.1155/2016/8106814>
- <sup>35</sup> M. Henriksson, G. Henriksson, L. A. Berglund and T. Lindström, *Eur. Polym. J.*, **43**, 3434 (2007), <https://doi.org/10.1155/2016/8106814>
- <sup>36</sup> J. Zeng, L. Liu, J. Li, J. Dong and Z. Cheng, *BioResources*, **15**, 3809 (2020), <https://doi.org/10.15376/biores.15.2.3809-3820>
- <sup>37</sup> S. Sankhla, H. H. Sardar and S. Neogi, *Carbohydr. Polym.*, **251**, 117030 (2021), <https://doi.org/10.1016/j.carbpol.2020.117030>
- <sup>38</sup> N. Hayat, H. Harahap and H. Nasution, *AIP Conf. Proc.*, (2019), <https://doi.org/10.1016/j.carbpol.2020.117030>
- <sup>39</sup> F. Ismail, N. E. A. Othman, N. A. Wahab and A. A. Aziz, *J. Oil Palm Res.*, **32**, 621 (2020), <https://doi.org/10.21894/jopr.2020.0057>
- <sup>40</sup> C. J. Huntley, K. D. Crews, M. A. Abdalla, A. E. Russell and M. L. Curry, *Int. J. Chem. Eng.*, **2015**, 1 (2015), <https://doi.org/10.1155/2015/658163>
- <sup>41</sup> H. Ji, Z. Xiang, H. Qi, T. Han, A. Pranovich *et al.*, *Green Chem.*, **21**, 1956 (2019), <https://doi.org/10.1039/C8GC03493A>
- <sup>42</sup> E. Abraham, B. Deepa, L. A. Pothan, M. Jacob, S. Thomas *et al.*, *Carbohydr. Polym.*, **86**, 1468 (2011), <https://doi.org/10.1016/j.carbpol.2011.06.034>
- <sup>43</sup> K. Trigui, C. De Loubens, A. Magnin, J. L. Putaux and S. Boufi, *Carbohydr. Polym.*, **240**, 116342 (2020), <https://doi.org/10.1016/j.carbpol.2020.116342>
- <sup>44</sup> W. Im, S. Lee, A. Rajabi Abhari, H. J. Youn and H. L. Lee, *Cellulose*, **25**, 3873 (2018), <https://doi.org/10.1007/s10570-018-1853-9>

- <sup>45</sup> F. Serra-Parareda, R. Aguado, Q. Tarrés, P. Mutjé and M. Delgado-Aguilar, *J. Clean. Prod.*, **313**, 27914 (2021), <https://doi.org/10.1016/j.jclepro.2021.127914>
- <sup>46</sup> K. L. Spence, R. A. Venditti, O. J. Rojas, Y. Habibi and J. J. Pawlak, *Cellulose*, **18**, 1097 (2011), <https://doi.org/10.1007/s10570-011-9533-z>
- <sup>47</sup> S. Kumneadklang, S. O-Thong and S. Larpiattaworn, *Mater. Today Proc.*, **17**, 1995 (2019), <https://doi.org/10.1016/j.matpr.2019.06.247>
- <sup>48</sup> S. Park, J. O. Baker, M. E. Himmel, P. A. Parilla and D. K. Johnson, *Biotechnol. Biofuels*, **3**, 10 (2010), <https://doi.org/10.1186/1754-6834-3-10>
- <sup>49</sup> W. Im, S. Lee, H. Park, H. L. Lee and H. J. Youn, *J. Korea Tech. Assoc. Pulp Pap. Ind.*, **48**, 195 (2016), <https://doi.org/10.7584/JKTAPPI.2016.12.48.6.195>
- <sup>50</sup> A. K. Veeramachineni, T. Sathasivam, S. Muniyandy, P. Janarthanan, S. J. Langford *et al.*, *Appl. Sci.*, **6**, 170 (2016), <https://doi.org/10.3390/app6060170>
- <sup>51</sup> H. P. S. Abdul Khalil, Y. Davoudpour, M. N. Islam, A. Mustapha, K. Sudesh *et al.*, *Carbohydr. Polym.*, **99**, 649 (2014), <https://doi.org/10.1016/j.carbpol.2013.08.069>
- <sup>52</sup> R. R. Ferreira, A. G. Souza, L. L. Nunes, N. Shahi, V. K. Rangari *et al.*, *Mater. Today Commun.*, **22**, 100755 (2020), <https://doi.org/10.1016/j.mtcomm.2019.100755>
- <sup>53</sup> B. G. Lopes, G. A. Faria, K. L. Maltoni, P. S. Rocha, A. P. B. Peixoto *et al.*, *Rev. Cienc. Agron.*, **52**, 1 (2021), <https://doi.org/10.5935/1806-6690.20210050>
- <sup>54</sup> T. Šoštarić, M. Petrović, J. Stojanović, M. Marković, J. Avdalović *et al.*, *Biomass Convers. Biorefin.*, **12**, 2377 (2020), <https://doi.org/10.1007/s13399-020-00766-2>
- <sup>55</sup> M. H. Sainorudin, M. Mohammad, N. H. A. Kadir, N. A. Abdullah and Z. Yaakob, *Solid State Phenom.*, **280**, 340 (2018), <https://doi.org/10.1007/s13399-020-00766-2>
- <sup>56</sup> P. Kaewprachu, C. Jaisan, S. Rawdkuen, W. Tongdeesoontorn and W. Klunklin, *Food Hydrocoll.*, **124**, 107277 (2022), <https://doi.org/10.1007/s13399-020-00766-2>
- <sup>57</sup> I. Gulati, J. Park, S. Maken and M.-G. Lee, *Fibers Polym.*, **15**, 680 (2014), <https://doi.org/10.1007/s12221-014-0680-3>
- <sup>58</sup> W. Li, B. Sun and P. Wu, *Carbohydr. Polym.*, **78**, 454 (2009), <https://doi.org/10.1016/j.carbpol.2009.05.002>
- <sup>59</sup> D. Trache, M. H. Hussin, C. T. H. Chuin, S. Sabar, M. R. N. Fazita *et al.*, *Int. J. Biol. Macromol.*, **93**, 789 (2016), <https://doi.org/10.1016/j.ijbiomac.2016.09.056>
- <sup>60</sup> M. El-Sakhawy, H. A. S Tohamy, A. Salama and S. Kamel, *Cellulose Chem. Technol.*, **53**, 667 (2019), <https://doi.org/10.35812/CelluloseChemTechnol.2019.53.65>
- <sup>61</sup> V. Gupta, D. Ramakanth, C. Verma, P. K. Maji and K. K. Gaikwad, *Biomass Convers. Biorefin.*, (2021), <https://doi.org/10.1007/s13399-021-01852-9>
- <sup>62</sup> A. F. Owolabi, M. K. M. Haafiz, M. S. Hossain, M. H. Hussin and M. R. N. Fazita, *Int. J. Biol. Macromol.*, **95**, 1228 (2017), <https://doi.org/10.1016/j.ijbiomac.2016.11.016>
- <sup>63</sup> P. H. F. Pereira, N. F. Souza, H. L. Ornaghi and M. R. de Freitas, *Ind. Crop. Prod.*, **150**, 112305 (2020), <https://doi.org/10.1016/j.indcrop.2020.112305>
- <sup>64</sup> C. M. Ewulonu, X. Liu, M. Wu and Y. Huang, *Cellulose*, **66**, 4371 (2019), <https://doi.org/10.1007/s10570-019-02382-4>
- <sup>65</sup> M. K. M. Haafiz, S. J. Eichhorn, A. Hassan and M. Jawaid, *Carbohydr. Polym.*, **93**, 628 (2013), <https://doi.org/10.1016/j.carbpol.2013.01.035>
- <sup>66</sup> K. J. Nagarajan, A. N. Balaji and N. R. Ramanujam, *Carbohydr. Polym.*, **212**, 312 (2019), <https://doi.org/10.1016/j.carbpol.2019.02.063>
- <sup>67</sup> W. R. Wan Daud and F. M. Djuned, *Carbohydr. Polym.*, **132**, 252 (2015), <https://doi.org/10.1016/j.carbpol.2015.06.011>
- <sup>68</sup> P. Yu, Y. Hou, H. Zhang, W. Zhang, S. Yang *et al.*, *BioResources*, **14**, 8923 (2019), [https://ojs.cnr.ncsu.edu/index.php/BioRes/article/view/BioRes\\_14\\_4\\_8923\\_Yu\\_Solubility\\_Effects\\_Carboxymethyl\\_Substituents/7174](https://ojs.cnr.ncsu.edu/index.php/BioRes/article/view/BioRes_14_4_8923_Yu_Solubility_Effects_Carboxymethyl_Substituents/7174)
- <sup>69</sup> D. Ciolacu, F. Ciolacu and V. I. Popa, *Cellulose Chem. Technol.*, **45**, 13 (2011), [https://cellulosechemtechnol.ro/pdf/CCT1-2\(2011\)/p.13-21.pdf](https://cellulosechemtechnol.ro/pdf/CCT1-2(2011)/p.13-21.pdf)
- <sup>70</sup> P. Rachtanapun and N. Rattanapanone, *J. Appl. Polym. Sci.*, **122**, 3218 (2011), <https://doi.org/10.1002/app.34316>
- <sup>71</sup> M. H. Hussin, N. A. Husin, I. Bello, N. Othman, M. A. Bakar *et al.*, *Int. J. Electrochem Sci.*, **13**, 3356 (2018), <https://doi.org/10.20964/2018.04.06>
- <sup>72</sup> B. I. M. Mejia, O. V. Kharissova and B. I. Kharisov, *Recent Pat. Nanotechnol.*, **13**, 151 (2019), <https://doi.org/10.2174/1872210513666190327152543>
- <sup>73</sup> M. I. G. Miranda, C. I. D. Bica, S. M. B. Nachtigall, N. Rehman and S. M. L. Rosa, *Thermochim. Acta*, **565**, 65 (2013), <https://doi.org/10.1016/j.tca.2013.04.012>
- <sup>74</sup> K. Harini and C. Chandra Mohan, *Int. J. Biol. Macromol.*, **163**, 1375 (2020), <https://doi.org/10.1016/j.tca.2013.04.012>
- <sup>75</sup> H. Yang, R. Yan, H. Chen, D. H. Lee and C. Zheng, *Fuel*, **86**, 1781 (2007), <https://doi.org/10.1016/j.fuel.2006.12.013>
- <sup>76</sup> J. I. Morán, V. A. Alvarez, V. P. Cyras and A. Vázquez, *Cellulose*, **15**, 149 (2008), <https://doi.org/10.1007/s10570-007-9145-9>
- <sup>77</sup> M. Yahya, Y. W. Chen, H. V. Lee, C. C. Hock and W. H. W. Hassan, *J. Polym. Environ.*, **27**, 678 (2019), <https://doi.org/10.1007/s10924-019-01373-7>
- <sup>78</sup> G. Chen, Z. Wang, L. Zhang, H. Liu, G. Wang *et al.*, *J. Eng. Fiber Fabr.*, **14**, (2019), <https://doi.org/10.1177/1558925019883451>
- <sup>79</sup> M. K. A. Abdul Razab, R. S. Mohd Ghani, F. A. Mohd Zin, N. A. A. Nik Yusoff and A. M. Noor, *J.*

- Nat. Fibers*, **1** (2021), <https://doi.org/10.1080/15440478.2021.1881021>
- <sup>80</sup> H. Li, H. Zhang, L. Xiong, X. Chen, C. Wang *et al.*, *Fiber. Polym.*, **20**, 975 (2019), <https://doi.org/10.1007/s12221-019-7717-6>
- <sup>81</sup> G. S. Hutomo, D. W. Marsemo, S. Anggrahini and Supriyanto, *Afr. J. Food Sci.*, **6**, 180 (2012), <https://doi.org/10.5897/AJFS12.020>
- <sup>82</sup> A. Kukrety, R. K. Singh, P. Singh and S. S. Ray, *Waste Biomass Valoriz.*, **9**, 1587 (2018), <https://doi.org/10.1007/s12649-017-9903-3>
- <sup>83</sup> S. Y. Park, S. Goo, H. Shin, J. Kim and H. J. Youn, *Cellulose*, **28**, 10291 (2021), <https://doi.org/10.1007/s10570-021-04151-8>
- <sup>84</sup> W. Chen, H. Yu, Y. Liu, P. Chen, M. Zhang *et al.*, *Carbohydr. Polym.*, **83**, 1804 (2011), <https://doi.org/10.1016/j.carbpol.2010.10.040>
- <sup>85</sup> S. Y. Oh, D. I. Yoo, Y. Shin and G. Seo, *Carbohydr. Res.*, **340**, 417 (2005), <https://doi.org/10.1016/j.carres.2004.11.027>
- <sup>86</sup> N. Amiralian, P. K. Annamalai, P. Memmott and D. J. Martin, *Cellulose*, **22**, 2483 (2015), <https://doi.org/10.1007/s10570-015-0688-x>
- <sup>87</sup> M. Rahimi Kord Sofla, R. J. Brown, T. Tsuzuki and T. J. Rainey, *Adv. Nat. Sci. Nanosci. Nanotechnol.*, **7**, 035004 (2016), <https://doi.org/10.1088/2043-6262/7/3/035004>
- <sup>88</sup> Z. Z. Chowdhury and S. B. A. Hamid, *BioResources*, **11**, 3397 (2016), <https://doi.org/10.15376/biores.11.2.3397-3415>